

# Non-Iterative Characteristics Analysis for Ramp Loading with a Window

Damian C. Swift,<sup>\*</sup> Dayne E. Fratanduono, Evan A. Dowling<sup>†</sup>, and Richard G. Kraus  
*Physics Division, Lawrence Livermore National Laboratory,  
7000 East Avenue, Livermore, California 94551, U.S.A.*

(Dated: November 6, 2018, revisions to February 12, 2019 – LLNL-JRNL-767557)

Ramp compression experiments are used to deduce the relation between compression and normal stress in a material, by measuring how a compression wave evolves as it propagates through different thicknesses of the sample material. The compression wave is generally measured by Doppler velocimetry from a surface that can be observed with optical or near-optical photons. For high-pressure ramp loading, the reflectivity of a free surface often decreases as it is accelerated by the ramp wave, and window materials transparent to the probing photons are used to keep the surface flatter and preserve its reflectivity. We previously described a method of analyzing ramp-wave data measured at the free surface which did not require numerical iteration. However, this method breaks down when the pressure at the surface changes and hence cannot be used for data taken with a finite-impedance window. We have now generalized this non-iterative analysis method to apply to measurements taken through a window. Free surfaces can be treated seamlessly, and the need for sampling at uniform intervals of velocity has been removed. These calculations require interpolation of partially-released states using the partially-constructed stress-compression relation, making them slower than the previous free-surface scheme, but they are still much more robust and fast than iterative analysis.

## I. INTRODUCTION

Ramp loading, or shockless compression, is used increasingly in equation of state (EOS) studies to measure the compressibility of matter along a continuous path that typically falls close to an isentrope [1]. Notable aspects of ramp loading experiments are that the sample is heated less than in shock loading, and a range of compressions are probed in a single experiment. Several methods have been used to apply ramp loading to a sample, including chemical explosives [2], pulsed magnetic fields [1], and laser pulses converted to pressure in a variety of ways [3–6].

Ramp loading does not generally induce perfectly isentropic compression in the sample because of irreversible processes such as plastic flow, although the ramp-loaded states can be corrected to find the isentrope if the constitutive response of the sample is known [7]. For convenience, we will use ‘isentropes’ to refer below to states obtained by ramp loading. Similarly, although the component of stress normal to the loading direction is the relevant value, and in general differs from the pressure because of material strength effects, for convenience we refer to normal stress as pressure.

The ramp wave is almost invariably analyzed from measurements of the velocity history at different distances into the sample, using interferometry of near-optical laser probes [8, 9]. Most materials are or become optically opaque, so the measurement must be performed

at a surface bounded by a transparent window or a vacuum. Generally, this interface introduces an impedance mismatch that complicates the measurement by reflecting waves back into the sample. The impedance mismatch must be taken into account when inferring the isentrope of the sample, and the inferred isentrope therefore depends on knowledge of the isentrope of the window. In this respect, a vacuum is preferable as its mechanical properties are perfectly defined. However, in practice it is found that the optical reflectivity of the free surface of the sample is often degraded, particularly at high pressures. Possible causes include changes in the inherent reflectivity of the material for instance by changes in conductivity caused by phase transitions, and by disruption of the surface as by ejecta from microscopic relief features such as machining grooves. In any case, transparent windows are employed widely as a palliative to confine the surface and maintain usable signal levels.

Ramp-loading data have generally been analyzed using an iterative technique in which the isentrope is assumed, and corrections are made repeatedly using the ramp data until the modified isentrope converges [10]. With such iterative refinement techniques, there is always a potential concern that the solution found may depend on the isentrope initially assumed, or on the parameters of the iterative scheme, or that the algorithm may fail to converge. We previously described a recursive, non-iterative analysis method [11] that gives the same result with greater stability and less computational effort, but was limited to free surface measurements sampled at uniform intervals of velocity. Here we generalize the previous method to windowed measurements; the generalized method of analysis is also valid for non-uniform sampling in velocity, which aligns more naturally with experimental data usually taken with uniform sampling in time.

<sup>†</sup>Current affiliation: University of Maryland – College Park, Maryland, U.S.A.

<sup>\*</sup>Electronic address: dswift@llnl.gov

The research described here was presented at the 2017 conference of the American Physical Society Topical Group on Shock Compression of Condensed Matter [12]. More detailed comparisons with hydrocode simulations were made subsequently, and are included below.

## II. ISENTROPE MEASUREMENT FROM RAMP LOADING

The stress-density relation for a material from a given initial state can be deduced from the evolution of a ramp load as it propagates through a sample of the material. The longitudinal sound speed generally varies with compression, so the evolution of a ramp in bulk matter is related directly to the sound speed and hence the normal stress. In a typical experimental configuration, the particle velocity history  $u(t)$  is measured at each of a set of steps of different thickness  $x$  (Fig. 1). If the window material through which each step is observed were a perfect impedance match to the sample, the particle speed measured at the interface at a given pressure would be the same as in the bulk material, and the sound speed  $c$  could be found from the time at which the particle speed  $u_p$  appeared at steps of different thickness,

$$c(u_p) = \Delta X / \Delta t(u_p; X), \quad (1)$$

However, usually the window is not a perfect impedance match, and forward-propagating characteristics from the ramp reflect back from the interface, perturbing the ramp and hence the velocity history measured at each step. The next section describes our new algorithm for correcting for the characteristics reflected from the impedance mismatch from the window.

As defined here,  $c$  is the longitudinal Lagrangian sound speed, i.e. with respect to uncompressed material. In the absence of elastic contributions,  $c$  is related to the sound speed calculated from the EOS,  $c_e = c\rho_0/\rho$  where  $\rho$  is the mass density and  $\rho_0$  its initial value. The normal stress  $p$  (or pressure, again if elasticity is neglected) can be calculated from  $c_e$  from the Riemann integral

$$p = \int \rho c_e du_p; \quad \rho = \int \frac{\rho}{c_e} du_p \quad (2)$$

where the EOS sound speed is

$$c_e \equiv \sqrt{B_s / \rho} \quad (3)$$

and  $B_s$  is the isentropic bulk modulus,  $\rho \partial p / \partial \rho|_s$ .

In the iterative analysis used previously [10], an estimate of the isentrope is used to correct for the reflected characteristics and hence obtain a new estimate of the isentrope. This process is repeated until a converged result is obtained. We showed previously [11] that, in the absence of a window, the correction for perturbing characteristics can be made in a non-iterative, deterministic way. Here we extend that analysis to the modified characteristics induced by a window.

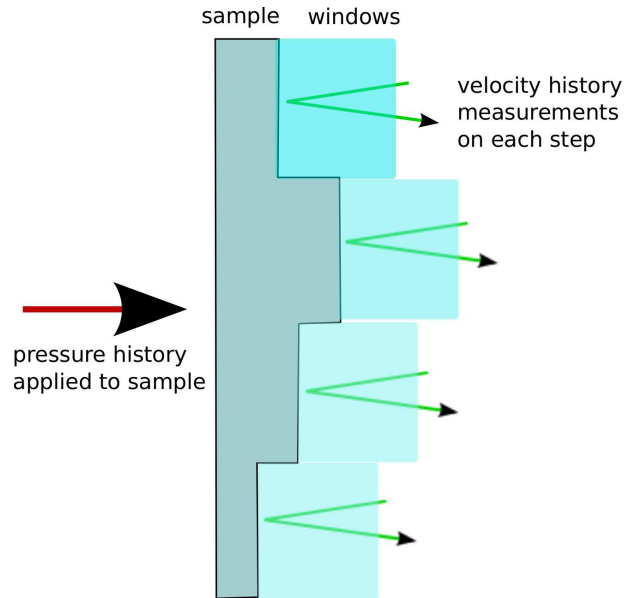


FIG. 1: Schematic of ramp wave experiment with window, used to deduce EOS.

## III. RAMP CHARACTERISTICS AT AN INTERFACE WITH A WINDOW

For experiments with a window to enable the isentrope of the sample to be deduced, the window's EOS must be known, along with its refractive index as a function of compression along its isentrope. The refractive index is often represented as a correction function that maps apparent particle speed (as if the refractive index were unity, as for a free surface) to the actual particle speed; physically, this correction involves a combination of the refractive index and the EOS [13]. At the interface, any given incoming characteristic has been affected by the reflection of all previous characteristics, but not by the reflection from any subsequent ones. If the window has a lower impedance than the sample, the reflected characteristics have a lower pressure than the subsequent incident characteristics, so the correction can be made deterministically using the corrected speed at the appropriate pressure that has already been explored. If the window has a higher impedance, the reflected characteristics have a higher pressure than the incident ones, so the correction must be made either by assuming the isentrope and iterating, or assuming a form of extrapolation from the previously-reconstructed region, which may be possible to adequate accuracy without iteration. From this point, the effect can be corrected for recursively, similarly to the free surface case [11].

The recursive correction proceeds by considering pairs of (position,time) points corresponding to successive forward-going characteristics  $i$  and  $i+1$  either at the interface or after correcting both for perturbations from the same number ( $j-1$ ) of backward-going reflective char-

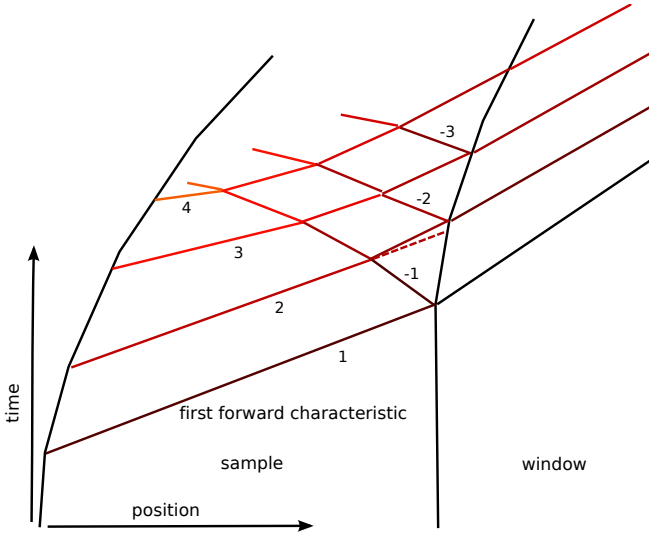


FIG. 2: Interaction between successive reflected characteristics. Successive forward-moving loading characteristics are numbered in sequence; negative numbers are the corresponding reflected characteristics. The dotted line represents the trajectory of characteristic 2 if it had not been perturbed by the reflection of characteristic 1.

acteristics, and deducing the intersection point between later characteristic and the next ( $j$ th) backward-going characteristic. In Lagrangian coordinates, i.e. the position of each element of the sample before loading starts, the next intersection is at

$$t_{i+1,j,s} = \frac{x_{i,j,s} - x_{i+1,j-1,s}}{2c_i} + \frac{t_{i,j,s} + t_{i+1,j-1,s}}{2} \quad (4)$$

$$x_{i+1,j,s} = x_{i+1,j-1,s} - c_i(t_{i+1,j,s} - t_{i+1,j-1,s}) \quad (5)$$

where the subscript  $s$  means that these equations are applied separately to data from each step. [11]. This correction can be made for each step, and the corresponding correction can be made for all subsequent characteristics (Figs 2).

Unlike the free surface case, the corrections for all intersecting left-going characteristics are applied to each right-going characteristic, and the corresponding intersection points stored, before the next right-going characteristic is processed. In contrast, for a free surface, every right-going characteristic can be processed to remove the effect of each left-going characteristics in turn, starting with the reflection from the surface and moving successively left [11]; there is no need to store data at the intersection of left-going characteristics once the correction for each has been made. The requirement to store more intermediate data is not a practical limitation for current or likely experiments, but it does make the software implementation more complicated.

As in the free surface case, after each characteristic has been corrected for the reflections from all preceding characteristics, its Lagrangian wave speed (again meaning with respect to uncompressed material) can be cal-

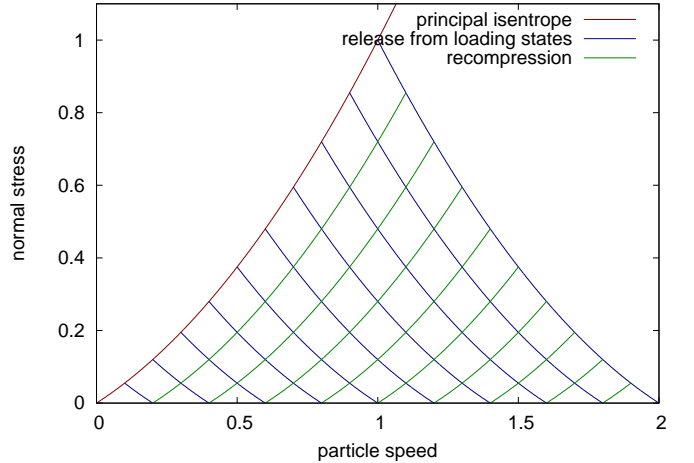


FIG. 3: Pressure-particle speed states occurring with free-surface velocity sampled at uniformly-spaced intervals.

culated from the corrected position-time data for two or more steps  $s$ :

$$c_i = \frac{\partial_s x_{i,i-1,s}}{\partial_s t_{i,i-1,s}} \quad (6)$$

where the partial derivative is used to represent linear fitting over the time – position data, or

$$c_i = \frac{x_{i,i-1,2} - x_{i,i-1,1}}{t_{i,i-1,2} - t_{i,i-1,1}} \quad (7)$$

for two steps.

In the free-surface analysis [11], we found that the algorithm required the free surface velocity history to be determined at equal increments of velocity, in common with preceding iterative algorithms [10]. This limitation may be inconvenient in practice, because experimental diagnostics of velocity typically determine the history at (at least approximately) equal increments of time. In a free-surface experiment, any characteristic reaching the surface travels at the zero-pressure longitudinal wave speed. With equal increments of velocity, the speed of characteristics further from the surface depends only on the number of interactions with lower-pressure characteristics, and thus the intersections between characteristics occur at the same set of velocities as are considered at the free surface, and the same set of pressures as are inferred along the isentrope [11] (Fig. 3). In the presence of a window, each reflected characteristic starts from the isentrope of the window at the pressure corresponding to the measured interface velocity. Thus the symmetry between right- and left-moving characteristics is broken, and neither the velocities nor pressures of intersections between characteristics fall into a set defined by its boundary values (Fig. 4).

In principle, the window case might be approached by interpolating velocities at the interface to find times corresponding to evenly-spaced velocities if it were a free

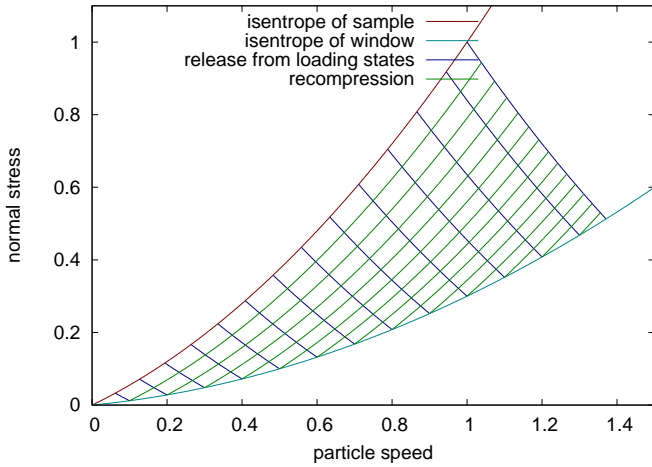


FIG. 4: Pressure-particle speed states occurring with velocity measured at interface with window.

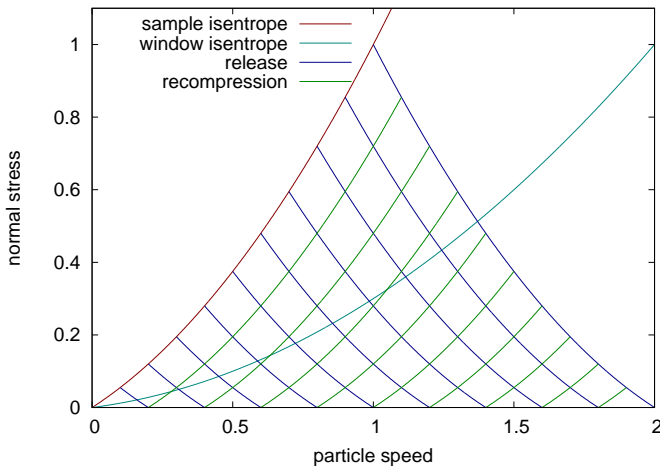


FIG. 5: Pressure-particle speed states along window isentrope, corrected so that effective free-surface velocity would be sampled at uniformly-spaced intervals.

surface. However, a complication is that forward- and backward-going characteristics would intersect the window isentrope at different times. At any point in the analysis, the fictitious sections of isentrope below the window isentrope would be translations of sections of the isentrope already recovered from the data, so this process would still be deterministic. (Fig. 5.)

However, we chose instead to develop a method to solve the problem of the skewed  $p - u$  mesh (Fig. 4) as this would also apply to the case of free-surface measurements at non-uniform intervals of velocity. Naively, one might think that, during the reconstruction of the isentrope of the sample, and even with a window of lower impedance than the sample, calculating the intersection from the previous point on the sample's isentrope and

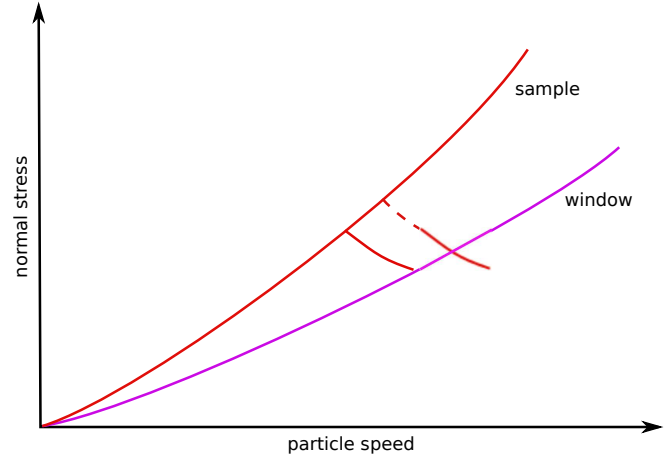


FIG. 6: Reflection and translation of partially-reconstructed isentrope to deduce next state along isentrope.

the last point on the backward-propagating characteristic involves extrapolating to the next higher pressure. However, the solution at the next point can be found by translating the release isentrope – the reflection of the partly-constructed isentrope – through the next state at the interface, and considering a symmetric compression-release cycle to determine the next state on the isentrope of the sample (Fig. 6). Translation is described by

$$\frac{\partial u_{\text{trans}}}{\partial u_{\text{win}}} = 1 + \left( \frac{\partial p}{\partial u} \right)_{\text{win}} \left( \frac{\partial p}{\partial u} \right)_{\text{sam}}^{-1} \quad (8)$$

evaluated at the pressure along the isentrope of the window at  $u_{\text{win}}$ . Then, the next state on the isentrope of the sample is at particle velocity increased by  $\Delta u = \Delta u_{\text{trans}}/2$  or

$$u = \frac{u_{\text{win}} + u_{\text{sam}}(p_{\text{win}})}{2}. \quad (9)$$

This procedure exactly reproduces the limiting cases of a free surface ( $p_{\text{win}} = 0 \quad \forall u_{\text{win}}$ ) and of an impedance-matched window.

As with our previous analysis, the step height only enters as a difference, so absolute step heights are irrelevant so long as the relative heights are known.

For the first characteristic, the analysis was performed completely as described above, and also with the zero-pressure value of longitudinal wave speed  $c_0$  supplied rather than calculated. This modification is appropriate for experimental data in which the uncertainty in  $c_0$  derived from low-pressure measurements may be significantly less than the value inferred from ramp data, which is some average of the values at zero pressure and the pressure of the first measurable acceleration.

#### IV. CALCULATION OF COMPRESSION AND NORMAL STRESS

The calculation of compression and normal stress is similar to the free surface case [11], except that the particle speed  $u_{\text{sam}}$  of states along the isentrope of the sample is obtained from the analysis above and not by dividing the free surface velocity by two. As before, the mass density changes with particle speed as

$$\frac{\partial \rho}{\partial u_p} = \frac{\rho}{c_e} \quad (10)$$

where the instantaneous longitudinal wave speed  $c_e = c\rho_0/\rho$ . The mass density can be integrated implicitly through the characteristics,

$$\rho_{i+1} = \rho_i \frac{1 + \Delta u_p / 2\bar{c}_e}{1 - \Delta u_p / 2\bar{c}_e} \quad (11)$$

where  $\Delta u_p$  is the difference in inferred particle velocity between characteristics  $i$  and  $i+1$ , and  $\bar{c}_e$  is the average longitudinal wave speed.

The corresponding rate of change of pressure through the characteristics is

$$\frac{\partial p}{\partial u_p} = \rho c_e, \quad (12)$$

which can be integrated numerically as

$$p_{i+1} = p_i + \Delta u_p \bar{\rho} \bar{c}_e. \quad (13)$$

#### V. ANALYSIS OF SIMULATED DATA

As a test case, we consider the analysis of simulated data for Cu ramp-loaded to 1 TPa, with a LiF window. The Cu and LiF were treated as behaving according to analytic EOS of the Grüneisen form [14]. The loading history was chosen, as in the test case for the free surface analysis [11], to be the ideal shape for all the characteristics to cross to form a shock at the same point in the material [15], if unperturbed by the effect of the window. The ideal shape was scaled so that the shock formation distance was  $200 \mu\text{m}$  (Fig. 7), with suitable steps being  $140$  and  $160 \mu\text{m}$ . Simulated experimental data were generated from continuum mechanics simulations of the velocity history at the surface of each step (Fig. 8). The simulations were performed using a Lagrangian hydrocode with a second-order predictor-corrector numerical scheme using artificial viscosity to stabilize the flow against unphysical oscillations [17]. The simulations used a spatial resolution of  $0.5 \mu\text{m}$ . Gaussian noise was added to the data in time or velocity.

The recursive analysis method was applied to the simulated data, produced at different resolutions, and with or without noise. At low pressures, the absolute discrepancy was small but the fractional discrepancy large because of the inaccuracy in determining the precise time at which

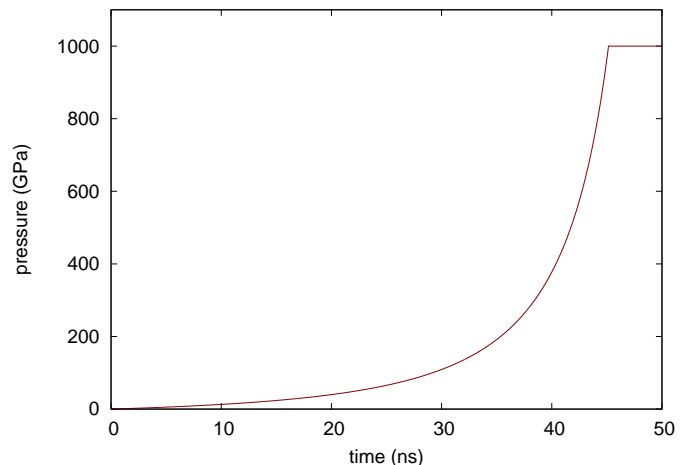


FIG. 7: Loading history applied to the Cu to generate simulated data.

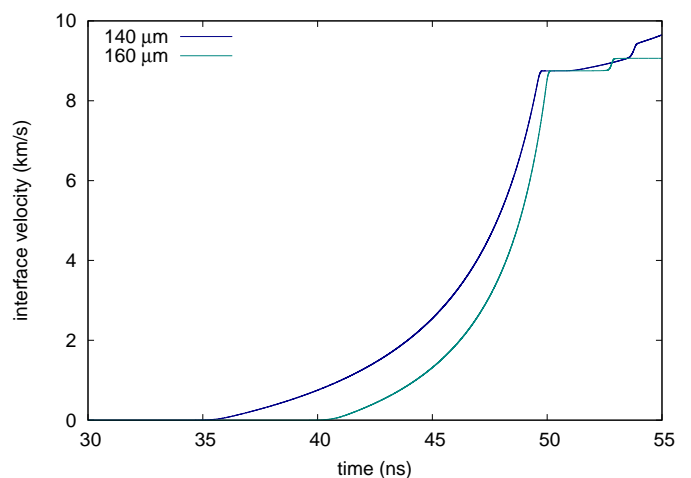


FIG. 8: Simulated velocity histories at the Cu/LiF interface for steps of different thickness, showing steepening of ramp wave.

acceleration stated. As the pressure along the isentrope rose, the fractional discrepancy fell rapidly to an asymptote of a fraction of a percent. The discrepancy was reduced when the simulated data were generated with finer spatial resolution, implying that part of the discrepancy was the finite precision of the hydrocode's numerical scheme. The discrepancy was also smaller when the interface velocity history was sampled at smaller intervals of time or velocity. (Fig. 9.)

We also tested the operation of the analysis algorithm on simulated data for a free surface, tabulated at non-uniform intervals of velocity. The algorithm reproduced the result obtained with the previous algorithm requiring uniform velocity intervals [11].

Compared with the recursive free surface analysis, the

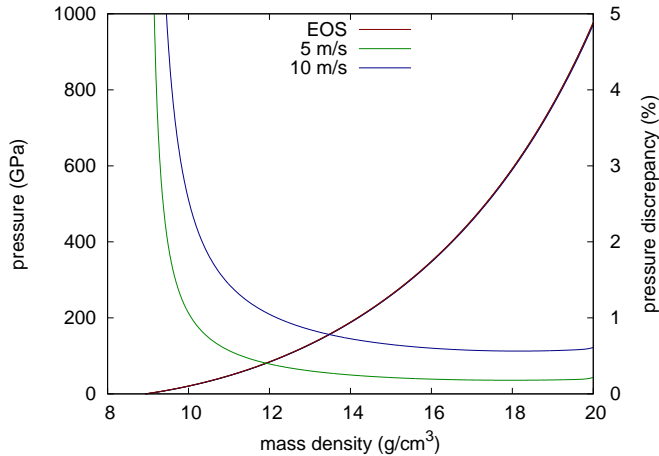


FIG. 9: Isentrope obtained by direct integration and by recursive characteristics analysis, with simulated data sampled at different intervals of velocity.

greater complexity of the window case increased the execution time significantly. For a typical experimental dataset, with the interface velocity sampled at a several hundred instants of time, the window algorithm took around 100ms, compared with  $\sim 10$ ms for the free surface algorithm. However, this is still several thousand times faster than the typical execution time of iterative schemes. For a high resolution dataset, with several thousand points from each step, the increase in speed would be proportionately larger.

## VI. CONCLUSIONS

We have developed a non-iterative algorithm – deterministic, and based on recursion over characteristics – for analyzing ramp-loading data, which gives the same results as the iterative algorithm generally used. No numerical problems were found in processing data with noise, though the data had to be filtered to be monotonic.

Comparing with simulated data representative of real experiments, the recursive algorithm was several orders of magnitude faster than the iterative algorithm, and performed more stably, giving a solution in cases where the iterative algorithm failed to converge. Unlike an iterative solution, the recursive algorithm does not require an estimate of the solution to be made as a starting condition, which is undesirable as it may bias the solution.

Even with a window, the deduction of a stress-density relation for a material from surface velocity measurements is inherently deterministic.

## VII. ACKNOWLEDGMENTS

Jean-Paul Davis prompted this study by asking whether recursion works with a window. We appreciate the support of Tom Arsenlis, Jim McNaney, and Dennis McNabb, for encouragement and funding via the National Ignition Facility High-Z campaign. This work was performed under the auspices of the U.S. Department of Energy by Lawrence Livermore National Laboratory under Contract DE-AC52-07NA27344.

- 
- [1] C.A. Hall, J.R. Asay, M.D. Knudson, W.A. Stygar, R.B. Spielman, T.D. Pointon, D.B. Reisman, A. Toor, and R.C. Cauble, *Rev. Sci. Instrum.* **72**, 3587 (2001).
  - [2] J.F. Barnes, P.J. Blewett, R.G. McQueen, K.A., Meyer, and D. Venable, *J. Appl. Phys.* **45**, 727 (1974).
  - [3] J. Edwards, K.T. Lorenz, B.A. Remington, S. Pollaine, J. Colvin, D. Braun, B.F. Lasinski, D. Reisman, J.M. McNaney, J.A. Greenough, R. Wallace, H. Louis, and D. Kalantar, *Phys. Rev. Lett.* **92**, 075002 (2004).
  - [4] D.C. Swift and R.P. Johnson, *Phys. Rev. E* **71**, 066401 (2005).
  - [5] R.F. Smith, J.H. Eggert, A. Jankowski, P.M. Celliers, M.J. Edwards, Y.M. Gupta, J.R. Asay, and G.W. Collins, *Phys. Rev. Lett.* **98**, 065701 (2007).
  - [6] D.K. Bradley, J.H. Eggert, R.F. Smith, S.T. Prisbrey, D.G. Hicks, D.G. Braun, J. Biener, A.V. Hamza, R.E. Rudd, and G.W. Collins, *Phys. Rev. Lett.* **102**, 075503 (2009).
  - [7] R.G. Kraus, J.-P. Davis, C.T. Seagle, D.E. Fratanduono, D.C. Swift, J.L. Brown, and J.H. Eggert, *Phys. Rev. B* **93**, 134105 (2016).
  - [8] Barker, L.M. and Hollenbach, R.E., *J. Appl. Phys.* **45**, 11 (1974).
  - [9] O.T. Strand, D.R. Goosman, C. Martinez, and T.L. Whitworth, *Rev. Sci. Instrum.* **77**, 083108 (2006).
  - [10] S.D. Rothman and J.R. Maw, *J. Phys. IV (Procs)*, **13A**, pp. 745750 (2006).
  - [11] D.C. Swift, D.E. Fratanduono, R.G. Kraus, and E.A. Dowling, submitted and [arXiv:1810.00929](https://arxiv.org/abs/1810.00929) (2018). The algorithm was also described in D.C. Swift, D. Fratanduono, and R.G. Kraus, presentation to American Physical Society Topical Conference on Shock Compression of Condensed Matter, <http://meetings.aps.org/Meeting/SHOCK15/Session/H5.3> (2015).
  - [12] E. Dowling, D. Fratanduono, and D.C. Swift, presentation to American Physical Society Topical Conference on Shock Compression of Condensed Matter, <http://meetings.aps.org/Meeting/SHOCK17/Session/Y6.4> (2017).
  - [13] D.H. Dolan, “Foundations of VISAR analysis,” Sandia National Laboratories report SAND2006-1950 (2006).
  - [14] D.J. Steinberg, *Equation of state and strength parameters for selected materials*, Lawrence Livermore National Laboratory report UCRL-MA-106439 change 1 (1996).
  - [15] D.C. Swift, R.G. Kraus, E.N. Loomis, D.G. Hicks, J.M. McNaney, and R.P. Johnson, *Phys. Rev. E* **78**, 066115 (2008).

- [16] D.C. Swift, J. Appl. Phys. **104**, 7, 073536 (2008).
- [17] Manual for LAGJ hydrocode V2.0 (Wessex Scientific and

Technical Services, Perth, 2016).